

# Advanced Workflows for Fluid Transfer in Faulted Basins.

Muriel Thibaut, Anne Jardin, Isabelle Faille, Françoise Willien, Xavier Guichet

▶ **To cite this version:**

Muriel Thibaut, Anne Jardin, Isabelle Faille, Françoise Willien, Xavier Guichet. Advanced Workflows for Fluid Transfer in Faulted Basins.. Oil & Gas Science and Technology - Revue d'IFP Energies nouvelles, 2014, 69 (4), pp. 573-584. 10.2516/ogst/2014016 . hal-01068236

**HAL Id: hal-01068236**
**https://ifp.hal.science/hal-01068236**

Submitted on 25 Sep 2014

**HAL** is a multi-disciplinary open access archive for the deposit and dissemination of scientific research documents, whether they are published or not. The documents may come from teaching and research institutions in France or abroad, or from public or private research centers.

L'archive ouverte pluridisciplinaire **HAL**, est destinée au dépôt et à la diffusion de documents scientifiques de niveau recherche, publiés ou non, émanant des établissements d'enseignement et de recherche français ou étrangers, des laboratoires publics ou privés.

*Oil & Gas Science and Technology – Rev. IFP Energies nouvelles*, Vol. 69 (2014), No. 4, pp. 573-584
Copyright © 2014, IFP Energies nouvelles
DOI: 10.2516/ogst/2014016

Dossier
*Geosciences Numerical Methods*
Modélisation numérique en géosciences

# Advanced Workflows for Fluid Transfer in Faulted Basins

Muriel Thibaut*, Anne Jardin, Isabelle Faille, Françoise Willien and Xavier Guichet

*IFP Energies nouvelles, 1-4 avenue de Bois-Préau, 92852 Rueil-Malmaison Cedex - France*
*e-mail: muriel.thibaut@ifpen.fr - anne.jardin@ifpen.fr - isabelle.faille@ifpen.fr - francoise.willien@ifpen.fr - xavier.guichet@ifpen.fr*

* Corresponding author

**Résumé** — **Méthodologie appliquée aux circulations des fluides dans les bassins faillés** — Une étude classique en modélisation en bassin en 3D se décompose en 3 étapes : la modélisation structurale et en faciès du bassin à l'âge actuel, la reconstruction structurale par restauration et enfin le couplage de ce modèle avec le calculateur direct pour une simulation en pression et température. Dans cette approche, la déformation tectonique est représentée par du cisaillement vertical le long des failles. Les propriétés de faille sont des propriétés de perméabilité intrinsèque homogène dans la zone de faille, elles traduisent le caractère drain ou barrière de la zone de faille.
Dans le cas où le bassin a subi des déformations tectoniques importantes, ces simplifications ne traduisent pas assez précisément la déformation tectonique. Ceci a un impact sur l'évaluation des pressions et la localisation des ressources en hydrocarbures.
Depuis quelques années, un nouveau calculateur direct pour la simulation en pression, température est développé à l'IFP Energies nouvelles. En parallèle, des outils logiciels ont été mis à disposition sur le marché pour offrir des scénarios de restauration 3D.
Dans cette publication, nous présentons les premières études couplant ces différents outils sur des exemples synthétiques de complexité croissante. Les exemples sont des cas inspirés de situation réelle et de déformation tectonique modérée.
Les deux cas d'application illustrent les résultats déjà obtenus et identifient les difficultés du couplage.

***Abstract*** — ***Advanced Workflows for Fluid Transfer in Faulted Basins*** — *The traditional 3D basin modeling workflow is made of the following steps: construction of present day basin architecture, reconstruction of the structural evolution through time, together with fluid flow simulation and heat transfers. In this case, the forward simulation is limited to basin architecture, mainly controlled by erosion, sedimentation and vertical compaction. The tectonic deformation is limited to vertical slip along faults. Fault properties are modeled as vertical shear zones along which rock permeability is adjusted to enhance fluid flow or prevent flow to escape.*
*For basins having experienced a more complex tectonic history, this approach is over-simplified. It fails in understanding and representing fluid flow paths due to structural evolution of the basin. This impacts overpressure build-up, and petroleum resources location.*
*Over the past years, a new 3D basin forward code has been developed in IFP Energies nouvelles that is based on a cell centered finite volume discretization which preserves mass on an unstructured grid and describes the various changes in geometry and topology of a basin through time. At the same time, 3D restoration tools based on geomechanical principles of strain minimization were made available that offer a structural scenario at a discrete number of deformation stages of the basin.*

*In this paper, we present workflows integrating these different innovative tools on complex faulted basin architectures where complex means moderate lateral as well as vertical deformation coupled with dynamic fault property modeling.*
*Two synthetic case studies inspired by real basins have been used to illustrate how to apply the workflow, where the difficulties in the workflows are, and what the added value is compared with previous basin modeling approaches.*

## INTRODUCTION

In view of the current context of oil and gas exploration, the discovery of new prospects in underexplored areas or residual reserves in mature areas will depend on our ability to work on deeper and structurally more complex targets such as deep offshore or deeply-buried reservoirs. All these new opportunities stretch the capabilities of currently available 3D basin exploration software, which can not provide accurate structural reconstruction of the basin coupled with the controlling physical processes that lead to the generation and migration of hydrocarbons.

Since 2000, 2D software tools like Thrustpack [1], Ceres2D [2] or TecLink2D [3, 4] exist that consider evolving geometry through geological time coupled with reconstruction of timing of hydrocarbon generation and expulsion. The basin geometry evolves through time as a result of sedimentation, erosion, salt or mud creeping and block displacement along faults. These displacements are accounted for using translation and rotation. Deformation modes are namely flexural slip and simple shear [1, 5-7]. 3D software like Temis3D [8] or Petromod3D [7] simulating fluid flow coupled with evolutionary geometry where paleogeometries are automatically computed by a method called "backstripping" or vertical decompaction [9]. These methods give a good approximation of the paleogeometries in a basin with limited amounts of faulting, small lateral throws and moderate tectonics. The fault complexity is greatly simplified: a fault is a zone modeled with a series of cells characterised in terms of facies and permeability but lateral fault offset is not considered. When tectonics yield faulted architecture, the method of backstripping is limited and too restrictive. In these cases, studies have demonstrated that a surface or volume restoration method must be applied to obtain a more accurate analysis of the structural deformation. For volume restoration, new approaches have been published using a mechanical or a geometric approach [10-13]. Both approaches give a kinematic restoration and a time-dependent 3D geometry which can be input to the forward simulator.

Since 2006, IFPEN has been developing a new basin simulator designed to handle moderately to highly deformed geometries and to better account for the impact of faults on fluid flow through time [14-18]. This new simulator computes compaction, heat transfer, and fluid flow migration. It is designed to be used after the definition of the present day basin architecture validated by restoration and section balancing techniques

In the first part of this paper, the basin modeling workflow adapted to such 3D approaches is described in three steps: firstly how to reconstruct the present day 3D geometry from structural interpretation, secondly how the paleogeometries are generated, and finally how faults are described in the new simulator.

Then two applications are presented. The first case study presents a simplified thrust belt with thrust layers and faulted geometries. The second case is derived from an extensional gravity basin focusing on fault kinematics and its impact on fluid flow. In the new basin simulator, efforts have been made to develop a solution that takes better into account the physical characteristics for the fault representation.

## 1 A 3D Advanced Basin Modeling Workflow

Our workflow separates the structural reconstruction from the forward basin modeling analysis. The advantage of this decoupled approach is that it is possible to use specific tools to perform each part of the workflow. The drawback of this decoupling is the lack of integration between the various steps of the workflow.

Our flow chart is composed of steps represented by a sequence of successive and discrete stages (*Fig. 1*). These steps are closely connected even if these are not assembled in the same software.

### 1.1 Step1: Present Day 3D Geometry of the Sedimentary Basin

The first step of the workflow (*Fig. 1a*) is the building of the present day 3D model [19]. In case of faulted geological structures, an important issue is the estimation of the correct layer and fault geometry in the depth domain. Efficient depth imaging and time to depth conversion of seismic data are obtained by an accurate velocity model through advanced inversion techniques and application of pre-stack depth migration [20].

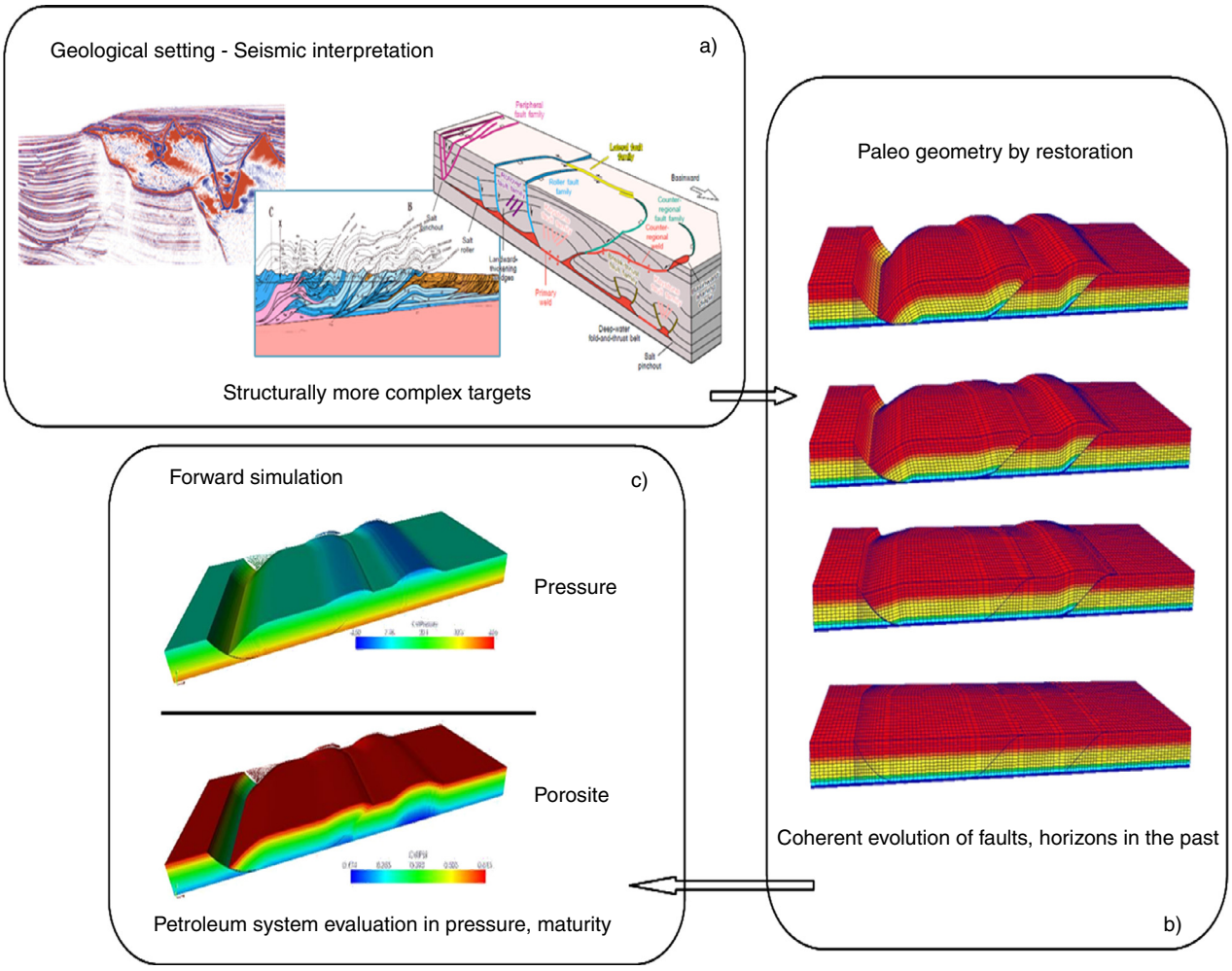



Figure 1

Proposed 3D basin modeling workflow. a) Present day 3D geometry of the sedimentary basin. Input data in structurally deformed environments: seismic cross sections, structural interpreted cross sections, 3D block diagrams with fault families. b) Basin history from palinspastic reconstruction. Illustration of paleo-geometries at various time steps of deformation of thrust units over a fixed unit. c) Forward simulation and fault description. Illustration of the coupling between paleo-geometries given in b) and forward simulations results of pressure and porosity at present day.

### 1.2 Step 2: Basin History from Palinspastic Reconstruction

The second step is the structural reconstruction through time (*Fig. 1b*). The structural model is built through successive backward geological deformations which is called restoration. Various surface restoration methods exist [18] and also some volumetric solutions [12, 13]. Surface algorithms unfold the layers from the present day structure back to the geometry at deposition time in a single step. With the volumetric approaches the structural scenario is given by a set of restored paleo-models. In the traditional 3D basin modeling workflow, backstripping is the algorithm to automatically compute the paleo-geometries. It is suitable for geologic settings dominated by normal deposition and erosion or for moderately extended basins with a limited structural complexity such that vertical shear is justified. But in areas with faulted basin architectures, the assumption of vertical decompaction is too restrictive, especially for describing lateral movements due to fault gliding. In this case, we have to consider a volume restoration which renders the integration more complex (*Fig. 1b*).

### 1.3 Step 3: Forward Simulation and Fault Description

The last step of the workflow (*Fig. 1c*) is the coupling of the time-dependent and evolutive grid of the basin with its fluid flow through dynamic fault property modeling.

Another point to mention is that, the forward simulation is based on an evolutive grid with specific requirements [6].

The traditional grids in 3D basin modeling software are structured meshes. Pressure regime and thermal history are fully coupled with the restoration [8]. A fault is a set of cells with facies properties and intrinsic permeability values. This approach allows both fluid migration within faults and faults as fluid barriers. Juxtaposition along faults is not taken into account.

In the new forward simulator, the basin is represented by a dynamic mesh which is described by step-by-step topologic (modification of the structure) and geometric (modification of coordinates) increments. Each layer is described by a set of cells of arbitrary shape, preferentially with hexahedral cells of reasonable aspect ratio. The mesh is a non structured mesh which evolves with the field of displacement in every spatial direction. This mesh can be continuous *via* deposition or erosion, or discontinuous for fault gliding and it is derived from volumetric restoration. The restoration builds an dynamic grid based on a discrete number of successive time steps, and the forward simulator operates a linear interpolation between these time steps to get a gradually deformed grid. In conclusion, the time-dependant mesh is more realistic, and physical properties are continuous through time.

In addition, the fault is geometrically represented as a boundary surface, with a left and right side and described by a set of faces (*Fig. 2a*). This representation is compatible with the paleo-re-construction of the model, as the two fault boundaries can slip relative to each other to follow fault kinematics and rock displacements through time. For the hydraulic behaviour, the fault is represented by a volume with a thickness, a spatially and temporally variable permeability, in which fluid flow can occur along and across the fault (*Fig. 2b*). The fault zone is not gridded explicitly with volumetric elements,. The width of the zone is too small compared to the basin scale and therefore tends to overestimate the volume zone. The fault width is taken into account as a parameter of the fluid flow model and is given as a property attached to the fault faces. Fault network is defined as a set of connections between surface meshes. With this definition, faults are zones of deformed rocks with flow properties. They are represented by a porous media and could act as a barrier or a conduit for fluid migration. Their lithologic characteristics differ from the surrounding host rock.

On this mesh with dynamic fault property modeling, the forward simulator computes multiphase flow coupled with compaction and heat transfer.

In the following examples, the dynamic mesh is obtained by two different approaches: the first by volumetric restoration [12, 13] (A), and the second by geometric modeling [11, 21, 22] (B).

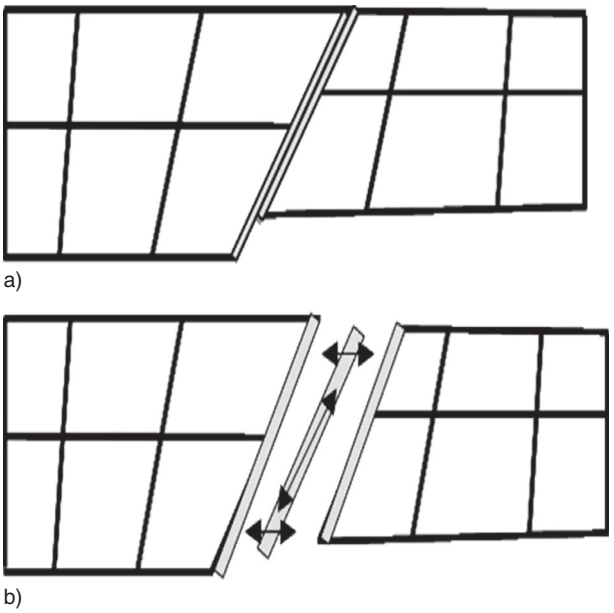



Figure 2

Fault zone between blocks. a) Representation of the fault surface with a right and left boundary. b) Representation of the fault surface with a right and left boundary and thickness. Arrows represent fluid flow along and across the fault zone.

(A) the kinematics is the result of a volumetric restoration constrained by the following assumptions:

- the basin is represented by a mesh conformable at faults and which compartmentalizes the basin into units that follow the geometry evolution due to deformation or fault activation;
- each layer is discretized into tetrahedra elements, and represents an homogeneous media. The mesh follows the stratigraphic deposition;
- only faults with significant throws are represented.

(B) the kinematics is given by a geometric approach based on the following assumptions:

- the basin is divided into several blocks delimited by faults and subdivided into layers;
- each layer is partitioned into a set of rigid quadrilateral elements which move by rotation and translation to preserve the thickness of the layer. The height of the edge of each elementary block is preserved vertically, in the case of the vertical shear, or perpendicular to the slipping support, in the case of the flexural slip;
- faults are considered as sliding support.

We will now illustrate the workflow with two synthetic examples of reasonable complexity inspired of real

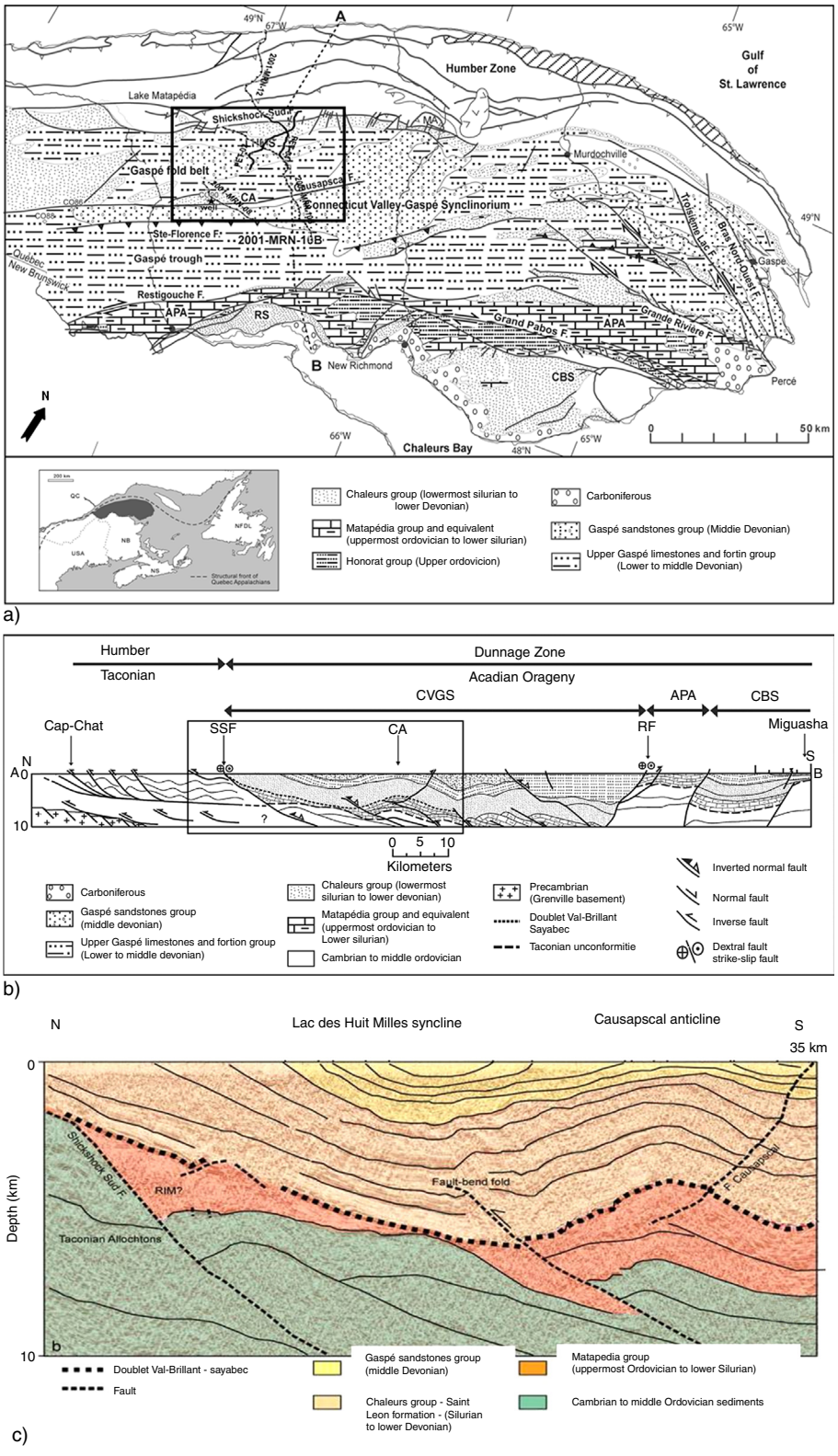



Figure 3

Geologic context of Gaspé peninsula in Quebec [4]. a) Simplified geologic map with stratigraphic units. The square box represents the studied area borded by the Shickshock and Causapscal faults. b) Structural interpretation based on the seismic line 2001-MRN-10B (represented by the cross-line A-B in dotted points in a)). The squared box represents the studied area. c) Zoom of the squared box in b). Detailed stratigraphic depth image of *Lac des Huit-Milles* synclinorium with interpreted lithofacies formation.

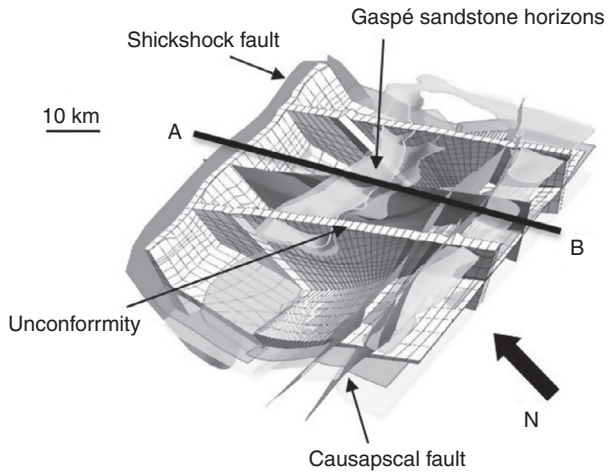



Figure 4

Gridded geological model of part of the Gaspé peninsula. a) View of the 3D present-day gridded model with the locations of Shickshock and Causapscal faults. The model fits with the isopachs given by the interpreted seismic data in Figure 3b. Erosion unconformities are well represented at the surface. The transparent horizons represent the different formations from the Gaspé sandstone group on the top of the Sayabec formation. Cross-line A-B from Figure 3a is located in the figure.

basins: the first one is used to demonstrate the feasibility of the complete workflow and the second one to appreciate the need of a fault description by a facies approach at basin scale.

## 2 3D Basin Modeling Workflow Applied to a Simplified Thrust Belt With Thrusted Layers and Faulted Geometries

### Geology

The first case study is inspired by the Gaspé Peninsula located in the northern part of the Canadian Appalachians (*Fig. 3a*) which presents a structurally complex geology characterized by two imbricate thrust belts [23-27]. At the surface, the contact between these thrust belts, is marked by the Shickshock Sud fault (*Fig. 3b*). To the south, the Causapscal fault is interpreted as a back-thrust [24, 28].

The central part of the Gaspé Peninsula delimits our study area (*Fig. 3a*). The structure "*Lac des Huits-Milles*" is a large open syncline 35 km wide that reaches 6.5 km depth at its core. It is limited to the North by the Shickshock Sud fault and to the south by the Causapscal fault (*Fig. 3b, c*). Based on the interpretation of 2D depth seismic images, a 3D block diagram of the central part of the Acadian Gaspé belt has been constructed (*Fig. 4*).

Figure 4 is the result of the first step of the workflow. The grid is a corner-point gridded model based on 14 horizons. Each layer is discretized into hexahedra, prisms and tetrahedra along the fault planes. The mesh is not coincident with the faults, in order to better describe the displacement along the fault planes. The 13 layers represent a very simplified stratigraphy of the basin because only the main stratigraphic formations are taken into account and considered as an homogeneous media without details of the heterogeneities in the formations. Each layer preserves the thickness of the formations on the interpreted seismic lines. The model size is 30 × 20 × 13 (7 800) cells. The lateral resolution is about 2 km. The present-day grid is coarse due to the limited number of cells. The structural deformation is limited to the main characteristics of the basin.

Figure 5 is the result of the second step of the workflow. It presents the evolution of the stratigraphic grid at 5 successive time-steps given by the volumetric restoration approach. The paleo-geometry is given at the end of each time step. This 4D grid reproduces properly the different stages of the deformation of the simplified basin (deposition, erosion, gliding along the faults). Compaction processes are not taken into account because the software is focused on geometry evolution and not on porosity reduction. To correct the value of depth, due to compaction, an outer "geometrical iterative loop" has been introduced where porosity is expressed through a lithology dependent law. At convergence of the iterations, this loop calibrates the rates of deposited sediments to satisfy the real thickness at present time.

The last step of the workflow is the thermal forward modeling of the basin through geological time. A constant basal heat flow of 50 $mW/m^2$ at the bottom of sediments has been used and a paleo-surface temperature of 15°C is assumed.

Figure 6a shows the burial history for a stratigraphic column of cells. The trend follows the geological history of the basin with a regular reduction of porosity with depth. Due to the over simplification of the model and the limited number of cells, even though the evolution of the input geometry is preserved, porosity curve does not reproduce in details the kinematics of the example. Figure 6b is the temperature history plot for the same stratigraphic column as in Figure 6a. Most formations have undergone a more or less continuous increase in burial.

At this stage, the results demonstrate the feasibility of the whole workflow, but there is no calibration against

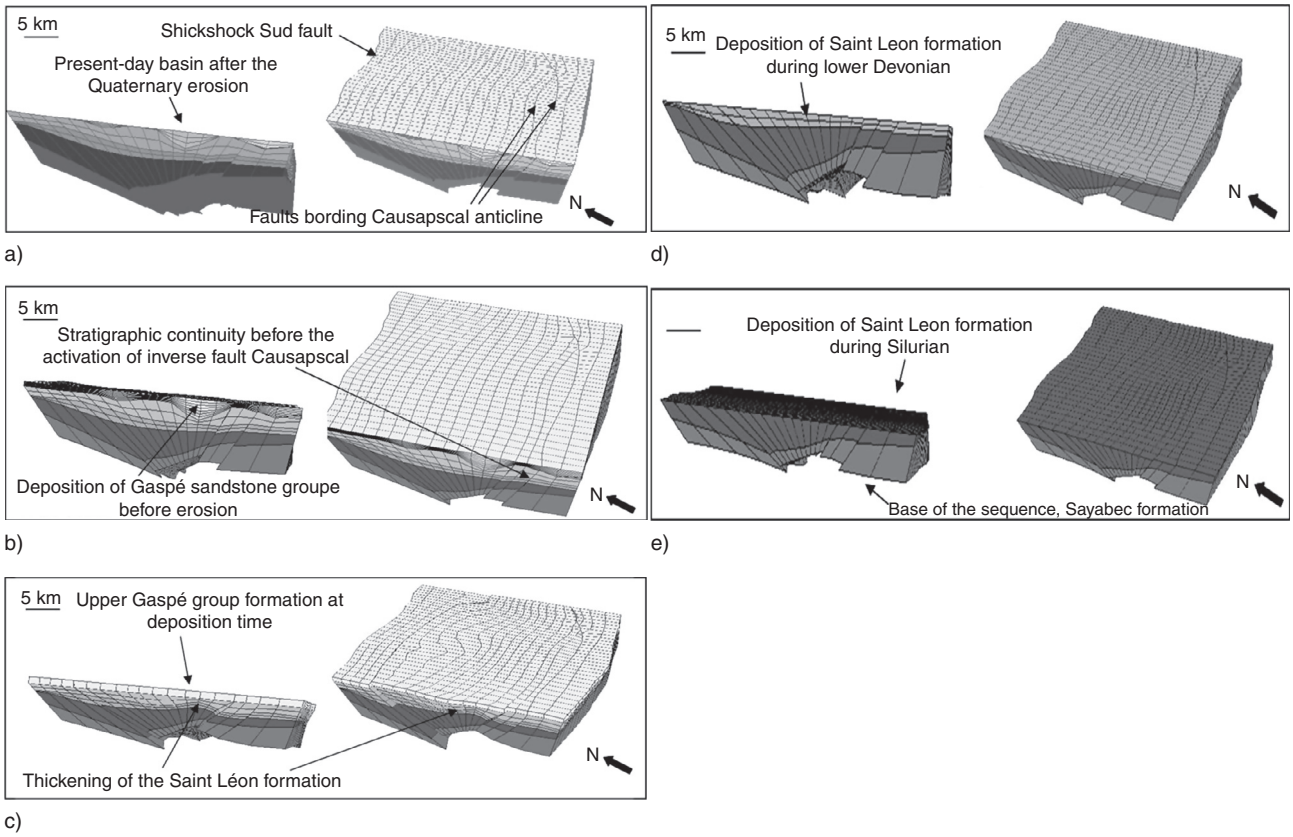



Figure 5

Representation of 3D paleogeometries resulting from the volumetric restoration at each deformation step, from youngest to oldest (section view on left and volume view on right). a) Geometry at present-day after the Quaternary erosion. b) Geometry before the Quaternary erosion and Acadian compressive phase, after the deposition of upper Gaspé group. c) Geometry after the deposition of the youngest rock unit in the syncline *Lac des Huit-Milles* during early Devonian times. d) Geometry after the deposition of Saint Leon formation after the extension phase in the Silurian period. e) Geometry during the extension phase after the deposition of Doublet Val-Brillant Sayabec formation, the oldest formation after the Taconian orogeny.

well data. The structural and stratigraphic geology of the area have been simplified to demonstrate the feasability of the workflow.

## 3 Advanced Fault Description for Fluid Flow Modeling: Example of a Basin Deformed by Gravity

To illustrate the impact of a more accurate characterisation of faults in basin modeling and its impact on fluid flow paths, a synthetic example inspired by geometries observed in the Gulf of Mexico [29] is presented in this part. It represents an extensional gravity system combining a listric fault in the shallow part of the slope with reverse faults at the toe of the slope.

Figure 7 illustrates the 3D model, showing a map view and a cross section. The chronology of displacement between the different units is the following: two units are displaced and thrust over the offshore domain by successive displacements in the dip direction. Figure 8 represents the folded structure with the reverse faults and the perfect slip on the normal fault.

The deformation history is described by layers undergoing flexural slip folding [22]. The lithofacies distribution used for modeling is an alternation of sand and shale layers. The structural history is composed of a normal deposition of sand and shale between 100 and 60 Ma (*Fig. 8a*), a sliding phase along the fault surfaces between 60 and 50Ma (*Fig. 8b*), and lastly a thrust episode between 50 and 45 Ma (*Fig. 8c*). The total number of cells equals to 35 200 cells.

This model is used to demonstrate the impact of the displacement on fluid flow, represented by the

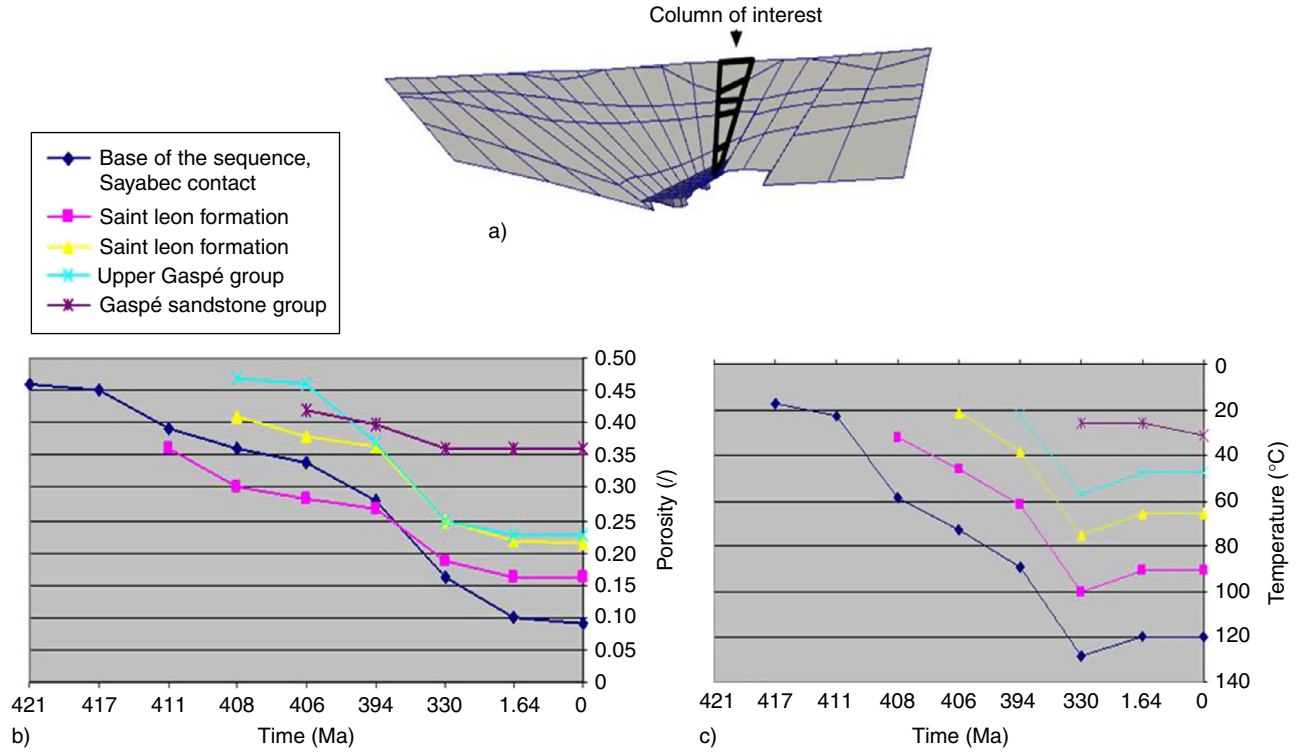



Figure 6

History of porosity and temperature for a stratigraphic column of the basin along a selected cross section of the model at present-day (*Fig. 5a*). a) The column of interest in the basin at present day is highlighted in bold line. b) Forward simulation in porosity and extraction of the history for the column of interest. c) Forward simulation in temperature and extraction of the history for the column of interest.

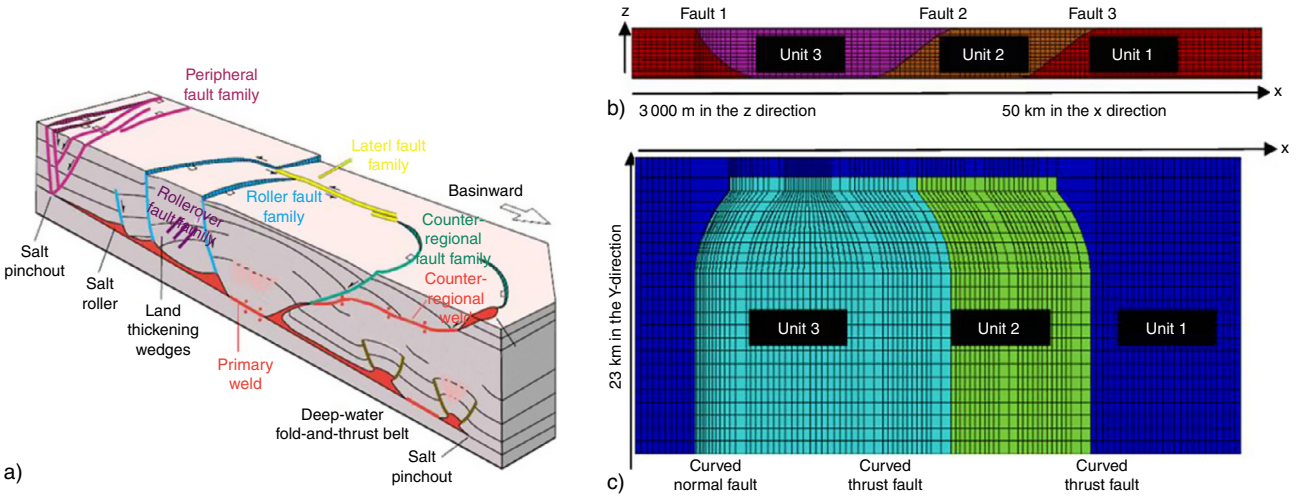



Figure 7

Structure with curved normal and thrust faults. a) Schematic representation of the model with normal faults in a structure [9], reprinted by permission of OGST. b) Representation of a 2D cross section describing the 3D model. c) Bird's-eye view of the initial 3D model and location of faults.

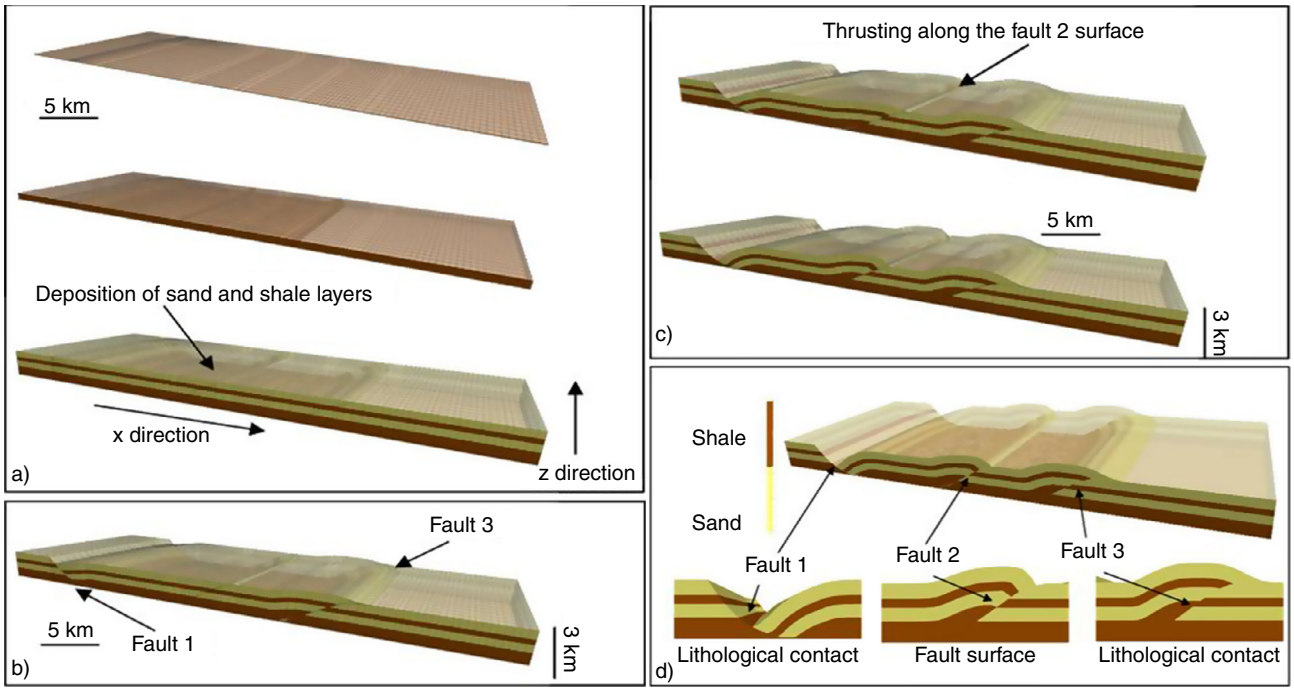



Figure 8

Volumetric deformation of the structure in Figure 7 through geologic time. Perspective views of the model after successive displacements. a) Sand and shale layers during normal deposition between 100 and 60 Ma. b) Sliding phase along the fault surfaces (fault 1 and fault 3) between 60 and 50 Ma. c) Thrusting phase between 50 and 45 Ma. d) Zoom of figure c) with the stratigraphic contacts along the faults. *X*-direction is the direction of deformation, and *Z*-direction of deformation, and *Z*-direction is the depth axis.

fault movement and how the impact is extended far from the faults into the surrounding host rock (*Fig. 8d*). It shows is the history of the reservoir connectivity along faults that will control the fluid flow through time.

Figure 9 presents the impact of the fault properties on fluid flow in the basin during time. Two scenarii are considered. In the first one, fault 2 is given an intrinsic permeability to behave as a baffle ($K = 0.01$ mD) and in the second one to behave as an impermeable barrier. For simplification, faults 1 and 3 are considered simply as contact surfaces, they do not have any properties. In this case, juxtaposition is the main driving factor for fluid flow direction and velocity.

In this example, from 60 to 58 Ma (*Fig. 9a*), fluid flow moves essentially by lithologic contrast and the fluid velocity is low. From 58 to 55 Ma (*Fig. 9b*), there is a contact between the sand layer and the top surface during the fault 1 activation. Flow is very important when fault 2 acts as a permeable interface, compared to an impermeable fault 2 which compartmentalizes the basin. From 55 to 51 Ma (*Fig. 9c*), activation of the fault 3 allows water circulation between the layer of sand and the top contact. Drainage across fault 3 is more important in the case of impermeable fault 2 due to the quantity of fluid trapped during the previous period. After 50 Ma (*Fig. 9d, e*), fluid velocity decreases because faults are less active and lithology contrasts less significant.

In Figure 10, the lithological distribution of the basin is modified by increasing the number of layers to demonstrate the impact of the fault model on overpressure distribution through time. It is a succession of 13 alternative sand-shale layers. Figure 10 represents the evolution of overpressure through time for a cross section on the central part of the model. Overpressure increases continuously through time to reach the highest values where the loading of sediment column is most important that means where units are thrusting over the basement. Overpressure is mainly

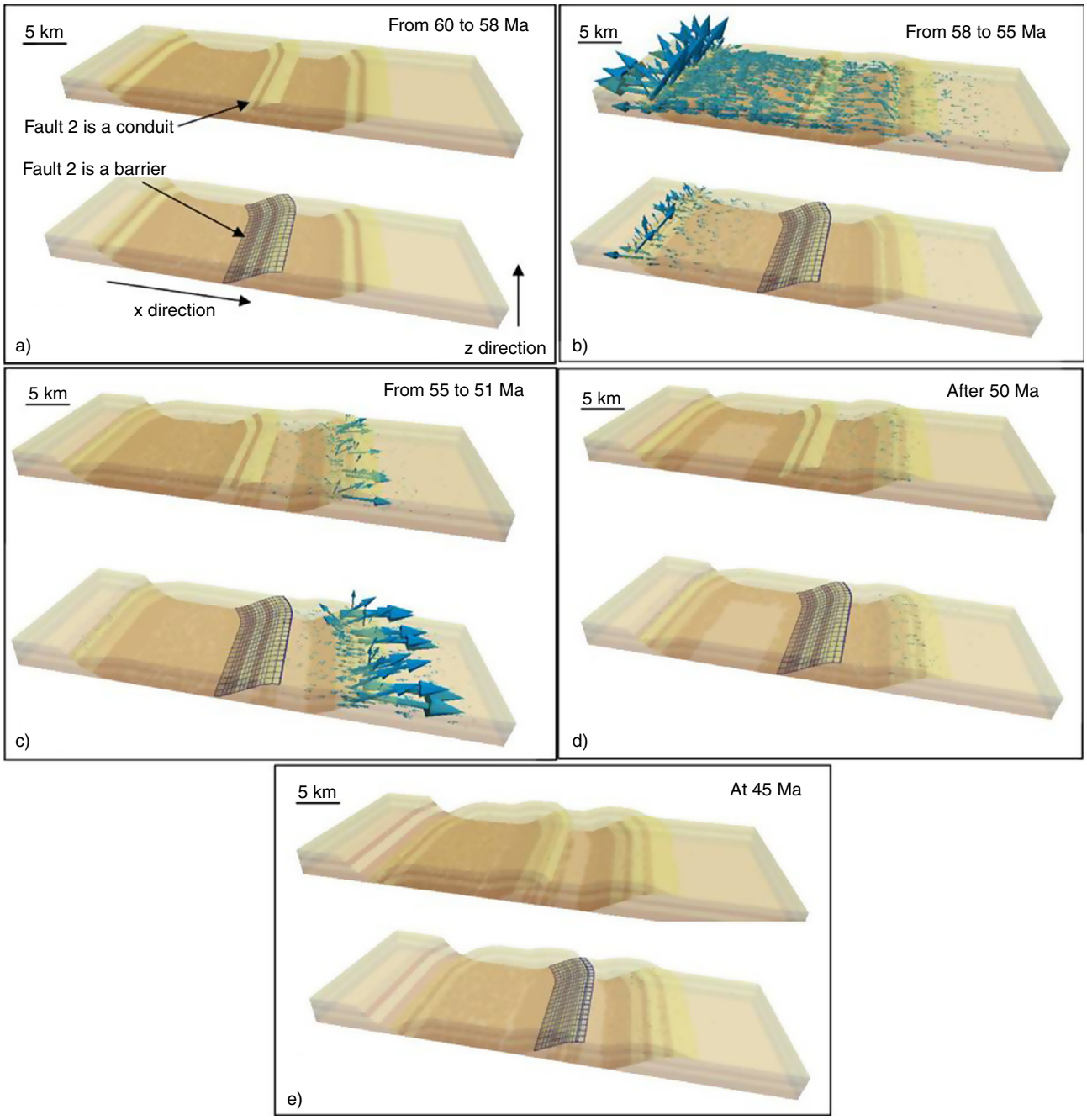



Figure 9

Forward simulation and impact of fluid flow during geologic history after the deposition of sand and shale layers. Top figures represent the scenario with fault 2 which acts as a conduit (transparent representation), and bottom figures as a barrier (gridded representation). Blue arrows represent water flow direction. The length of the arrow represents the absolute norm of the water flow between 0 and 3 000 m/Ma. a) Low fluid velocity from 60 and 58 Ma. b) Hydrodynamics increased due to the contact between sand layer and the contact surface from 58 to 55 Ma. c) Hydrodynamics due to the activation of fault 3 from 55 to 51 Ma. d, e) Lower hydrodynamics due to low lithologic contrast and less activity from the faults.

concentrated in the shaly layers and the fault parametrization (fault 2 is a barrier) is one of the controlling factor for this pressure increase.

Our results demonstrate the potential of a more accurate fault property and geometry modeling to explain fluid transfer and overpressure. The structural and

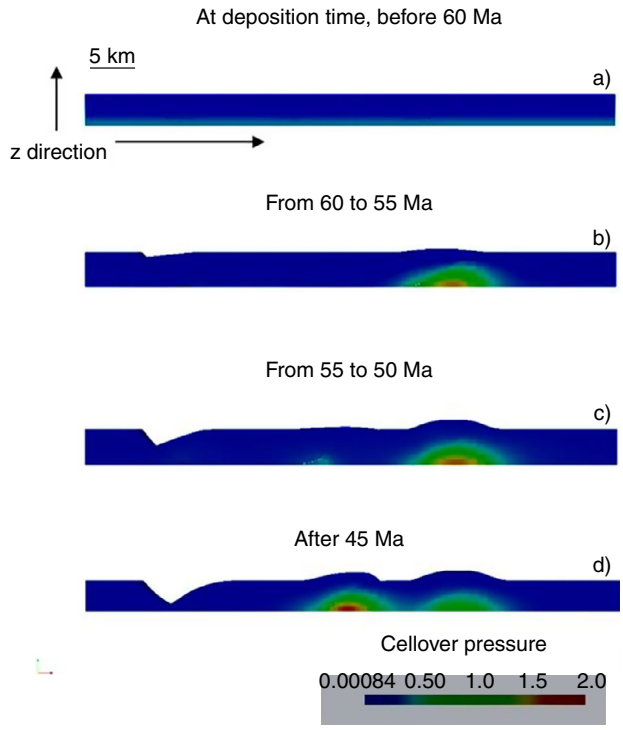



Figure 10

3D model in overpressure at different time steps. The number of time steps is related to Figure 9. Illustrations are given on a cross-section. Overpressure is given in MPa.

stratigraphic representation of our examples have been highly simplified which is a necessary first step to subsequently address more realistic 3D basin models.

## CONCLUSIONS

Targeting new resources in deeper and structurally more complex geological environments requires an advanced basin modeling workflow to describe fluid transfer due to fault activity. In this paper, we present an advanced basin workflow integrating existing innovative tools [13, 14]. They represent solutions towards the development of a fully coupled 3D approach of the structural reconstruction with forward simulation.

Using two greatly simplified examples from compressional and extensional settings, results have demonstrated that such a basin workflow can be well established and that a fault model is possible on unstructured grids at basin scale.

Beside the evaluation of the workflow, we have introduced an innovative 4D grid concept which is a major step forward that allows to follow continuously deforming basin architecture in faulted environments, including displacement along the faults, and accounting for fluid flow coupled with relative displacement of the fault walls.

More work needs to be done to cover a large range of complex structural situations on a continuously evolving grid. We are only at the beginning by using synthetic examples that have been inspired by real cases and many difficulties still exist to make this workflow fully operational in natural cases.

## ACKNOWLEDGMENTS

The authors would like to thank IFPEN for permission to publish this paper. Many thanks to W. Sassi and J. Wendebourg for their constructive comments. The authors would like to thank C. Souque, F. Roure for interesting discussions, G. Rodet for his participation in the generation of some results published in this paper, C. Sulzer in the building of the Gaspé model, M. Guiton for his help in the use of the prototype KINE3D-3. The work done on the Gaspé belt has been done in the framework of a methodological project between IFPEN (France), INRS (Canada) and Petrolia (Canada). We wish to thank them for their participation and support from the beginning of the collaboration. We thank colleagues from Petrolia and MRNFQ (*Ministère des Ressources Naturelles et Faune du Québec*) for giving their kind permission to present this material and for providing the data. The software used for the modeling is Gocad from Paradigm with the plugins KINE3D1-2-3.

## REFERENCES

1 Sassi W., Graham R., Gillcrist R., Adams M., Gomez R. (2007) The impact of deformation timing on the prospectivity of the Middle Magdalena sub-thrust, Colombia, Ries A. C., Butler R.W.H., Graham R.H. (eds), *Deformation of the Continental Crust: The Legacy of Mike Coward,* GSL Special Publications **272**, 473-498.

2 Schneider F. (2003) Basin Modeling in Complex Area: Examples from Eastern Venezuelan and Canadian Foothills, *Oil & Gas Science and Technology* **58**, 2, 313-324.

3 Baur F., Di Benedetto M., Fuchs T., Lampe C., Sciamanna S. (2009) Integrating structural geology and petroleum systems modeling – A pilot project from Bolivia's fold and thrust belt, *Marine and Petroleum Geology* **2**, 4, 573-579.

4 Lampe C., Kornpihla K., Sciamanna S., Zapatab T., Zamorab G., Varadéb R. (2006) Petroleum systems modeling in tectonically complex areas — A 2D migration study from the Neuquen Basin, Argentina, *Journal of Geochemical Exploration* **89**, 1-3, 201-204.

5 Samson P. (1996) Equilibrage de structures géologiques 3D dans le cadre du projet GOCAD, *PhD Thesis*, Institut National Polytechnique de Lorraine, Nancy.

6 Gibergues N., Thibaut M., Gratier J.-P. (2009) Three-dimensional kinematic modeling of reversible fault and fold development, *AAPG Bulletin* **93**, 1691-1704.

7 Hantschel T., Kauerauf A. (2009) *Fundamentals of Basin and Petroleum Systems Modeling*, Springer-Verlag, Heidelberg.

8 Schneider F., Wolf S., Faille I., Pot D. (2000) A 3D-Basin Model for Hydrocarbon Potential Evaluation: Application to Congo Offshore, *Oil & Gas Science and Technology* **55**, 1, 3-13.

9 Perrier R., Quiblier J. (1974) Thickness changes in sedimentary layers during compaction history, *Am. Assoc. Pet. Geol. Bull.* **58**, 3, 507-520

10 Cornu T., Schneider F., Gratier J.-P. (2003) 3D discrete kinematic modeling applied to extensional and compressional tectonics, *Geological Society of London Special Publication* **212**, 285-294.

11 Divies R. (1997) Foldis: un modèle cinématique de bassins sédimentaires par éléments discrets associant plis, failles, érosion/sédimentation et compaction, *PhD Thesis*, Université Joseph Fourier, Grenoble, France.

12 Maerten L., Pollard D.D., Maerten F. (2001) Digital mapping of three dimensional structures of Chimney Rock fault system, Central Utah, *Journal of Structural Geology* **23**, 585-592.

13 Moretti I., Lepage F., Guiton M. (2006) Kine3D: a new 3D restoration method based on a mixed approach linking geometry and geomechanics, *Oil & Gas Science and Technology* **61**, 2, 277-289.

14 Faille I., Thibaut M., Cacas M.C., Willien F., Wolf S., Agelas L., Pegaz-Fiornet S. (2013) Modeling fluid flow in faulted basins. In review.

15 Thibaut M., Sulzer C., Jardin A., Bêche M. (2007) ISBA3D: A Methodological Project for Petroleum System Evaluation in Complex Areas, *AAPG Database*, Search and Discovery Article #40269.

16 Thibaut M., Faille I., Willien F., Have P., Pegaz-Fiornet S., Rodet G. (2012) Building Better Integration between Structural Complexity and Basin Modeling, *AAPG Database, Search and Discovery* Article #40891.

17 Tunc X., Faille I., Gallouët T., Cacas M.-C., Havé P. (2012) A model for conductive faults with non-matching grids, *Computational Geoscience* **16**, 277-296.

18 Gibbs A. (1983) Balanced cross-section construction from seismic sections in areas of extensional tectonics, *Journal of Structural Geology* **5**, 153-160.

19 Mallet J.L. (2002) *Geomodeling*, *Applied Geostatistics*, Oxford University Press.

20 Robein E. (2003) Velocities, Time-imaging and depth-imaging: Principles and methods, *EAGE Publications*, BV.

21 Faille I., Havé P., Thibaut M., Willien F., Rudkiewicz J.L., Cacas M.C. (2009) A new 3D simulator for modeling fluid and heat flow in faulted basins, *AAPG Search and Discovery* Article #90091.

22 Gratier J.-P., Guillier B. (1993) Compatibility constraints on folded and faulted strata and calculation of the total displacement using computational restoration, *Journal of Structural Geology* **15**, 391-402.

23 Kirkwood D., Lavoie M., Marcil J. (2004) Structural style and hydrocarbon potential in the Acadian foreland thrust and fold belt, Gaspé Appalachians, Canada, Swennen R., Roure F., Granath J. (eds), *Deformation, fluid flow, and reservoir appraisal in foreland fold and thrust belts*, *AAPG Hedberg Series* **1**, 412-430.

24 Bourque P.A., Malo M., Kirkwood D. (2001) Stratigraphy, tectono-sedimentary evolution and paleogeography of the post-Taconian - Pre-Carboniferous Gaspé Belt: an overview, *Bulletin of Canadian Petroleum Geology* **49**, 2, 186-201.

25 Malo M., Kirkwood D. (1995) Faulting and progressive strain history of the Gaspé Peninsula in post-Taconian time: A review, Hibbard J.P., van Staal C.R., Cawood P. A. (eds), Current Perspectives in the Appalachian- Caledonian Orogen, *Geological Association of Canada* **41**, 267-282.

26 Morin C., Laliberté J.-Y. (2002) The unexpected Silurian-Devonian structural style in western Gaspé – New insight for promising hydrocarbon plays, *Canadian Society of Petroleum Geology, Jubilee Meeting, Calgary 2002*, **240**.

27 Sacks P.E., Malo M., Trzcienski Jr, Pincivy A., Gosselin P. (2004) Taconian and Acadian transpression between the internal Humber Zone and the Gaspé Belt in the Gaspé Peninsula: tectonic history of the Shickshock Sud fault zone, *Canadian Journal of Earth Sciences* **41**, 635-653.

28 Bêche M. (2008) Architecture structurale de la ceinture de Gaspé (Canada) : imagerie sismique intégrée et application à l'évaluation pétrolière, *Ph. Thesis*, Université Laval, Québec, Canada and Université de Cergy-Pontoise, France.

29 Rowan M., Jackson P.-P., Trudgill B. (1999) Salt related fault families, and fault welds in the northern Gulf of Mexico, *AAPG Bulletin* **83**, 1454-1484.

*Manuscript accepted in March 2014*
*Published online in June 2014*

*Copyright © 2014 IFP Energies nouvelles*

*Permission to make digital or hard copies of part or all of this work for personal or classroom use is granted without fee provided that copies are not made or distributed for profit or commercial advantage and that copies bear this notice and the full citation on the first page. Copyrights for components of this work owned by others than IFP Energies nouvelles must be honored. Abstracting with credit is permitted. To copy otherwise, to republish, to post on servers, or to redistribute to lists, requires prior specific permission and/or a fee: request permission from Information Mission, IFP Energies nouvelles, revueogst@ifpen.fr.*